

Characteristics of multiscale vortices in the simulated formation of Typhoon Durian (2001)

Yaping Wang,^{1,2} Xiaopeng Cui^{1,3} and Yongjie Huang^{1,2*}

¹Key Laboratory of Cloud-Precipitation Physics and Severe Storms (LACS), Institute of Atmospheric Physics, Chinese Academy of Sciences, Beijing, China

²University of Chinese Academy of Sciences, Beijing, China

³Collaborative Innovation Center on Forecast and Evaluation of Meteorological Disasters, Nanjing University of Information Science & Technology, Nanjing, China

*Correspondence to:

Y. Huang, Key Laboratory of Cloud-Precipitation Physics and Severe Storms (LACS), Institute of Atmospheric Physics, Chinese Academy of Sciences, No. 40 Huayanli, Chaoyang District, Beijing 100029, China.
E-mail: huangyj@mail.iap.ac.cn

Abstract

The formation of Typhoon Durian (2001) was simulated well by the Weather Research and Forecasting model. The vorticity field was separated into three scales: small scale ($L < 30$ km), intermediate scale ($30 \text{ km} < L < 120 \text{ km}$), and system scale ($L > 120 \text{ km}$), where L is wavelength. During the formation, small-scale vorticity anomalies, associated with convection, aggregated radially inward and rotated anticlockwise. The system-scale vorticity field presented a distinct mid-level vortex before genesis, and then a well-organized low-level vortex. The spectral power of the low-level vorticity at the small scale barely changed, while that at the system scale continued to grow steadily. The vorticity growth or spin-up of the near-surface tropical cyclone embryo was mainly due to the convergence of vertical vorticity flux at the planetary boundary layer. The positive (negative) effect of vorticity flux convergence at lower (middle-to-upper) levels appears to cause the shift of system-scale vorticity center from the middle to lower troposphere.

Received: 12 September 2015
Revised: 23 June 2016
Accepted: 6 July 2016

Keywords: tropical cyclogenesis; multiscale vortices; WRF model; Typhoon Durian

I. Introduction

Tropical cyclone (TC) formation, involving interactions among multiple spatial- and temporal-scale systems, is a very important aspect of TC research. Large-scale environmental conditions and physical factors associated with TC formation have been studied for a long time (Palmen, 1948; Riehl, 1948; Gray, 1968; Cheung, 2004; Zhang and Cui, 2013). Gray (1968) and McBride and Zehr (1981) proposed six factors favorable for TC formation: sufficient ocean thermal energy with sea surface temperature over 26 °C; enhanced mid-troposphere relative humidity; a deep layer of conditional instability; weak to moderate vertical wind shear; displacement by at least 5° away from the Equator; and cyclonic low-level relative vorticity. Besides, interactions among large-scale circulation, mesoscale convective activities, and convective-scale systems during TC genesis have also received considerable attention (Zhang and Bao, 1996a, 1996b; Bister and Emanuel, 1997; Ritchie and Holland, 1997, 1999; Zhang *et al.*, 2010; Fang and Zhang, 2011; Lu *et al.*, 2012; Park *et al.*, 2015). All of these lines of enquiry can be summed up into a key issue: how mesoscale vortices and small-scale deep convection organize to create a system-scale TC vortex.

In terms of TC development, several theories have been proposed, such as the convective instability of the second kind (Charney and Eliassen, 1964) and wind-induced surface heat exchange (Emanuel, 1986; Rotunno and Emanuel, 1987), both of which require

a preexisting initial low-pressure vortex with a certain intensity. More recently, a number of theories describing TC-scale vorticity enhancement have been proposed. Bister and Emanuel (1997) postulated a pathway for the development of Hurricane Guillermo, based on observations and numerical simulation; that is, a mid-level mesoscale convective vortex (MCV) expanded downward and, later, a near-surface cyclone with a warm core developed. This kind of approach is referred to as ‘top-down’ thinking. In contrast, another hypothesis, following ‘bottom-up’ thinking, emphasizes the key role of surface-based convection in the genesis process. Several hypotheses on the organizational mechanisms of small-scale deep convection have also been proposed. Montgomery *et al.* (2006) and Hendricks *et al.* (2004) suggested that vortical hot towers (VHTs) contribute to system-scale spin-up via the aggregation and merger of VHT-induced vorticity anomalies, as well as via diabatic heating. Lu *et al.* (2012) and Zhang *et al.* (2012) suggested that a system-scale vortex forms with the merger and aggregation of VHTs as one of the possible mechanisms, while Fang and Zhang (2011) (FZ11 hereinafter) pointed out that system-scale vorticity grows through diabatic heating-induced convergence of environmental and convectively generated vorticity. Above all, TC genesis remains an open question involving multiscale systems from several kilometers to several hundred kilometers.

TCs forming over the northwest Pacific Ocean, including the South China Sea (SCS), often impose

serious and rapidly occurring disasters upon the dense population of south and southeast China. Therefore, examination of TC formation processes is very important. With the development of remotely measured observations including those obtained from radar, satellites, aircraft and surface stations, multiscale vortex features, and their evolutions during TC genesis have begun to be revealed, especially those taking place in the Western Pacific and Atlantic (Reasor *et al.*, 2005; Sippel *et al.*, 2006; Houze *et al.*, 2009; Davis and Ahijevych, 2012). However, observations remain inadequate in the SCS region. Thus, high-resolution numerical simulations are a very useful tool to spatiotemporally resolve the dynamics and thermodynamics of TC formation processes in detail. In this context, this study focused on the characteristics and evolution of multiscale vortices, as well as how they related to the genesis of Typhoon Durian (2001) in the SCS, using numerical simulation. The next section introduces Typhoon Durian (2001) and describes how we verified the simulation using available observations. Section 3 reports the multiscale features during Durian's genesis through the scale-separation method.

2. Simulation of Durian

2.1. Review of TC Durian (2001)

Durian was recorded to initially generate as a tropical depression (TD, with winds of $10.8\text{--}17.1\text{ m s}^{-1}$ in China) at $(117^\circ\text{E}, 16^\circ\text{N})$ within the monsoon trough at 0600 UTC on 29 June 2001 in the middle region of the SCS. After that, Durian moved northwest and developed into a tropical storm (TS, with winds of $17.2\text{--}24.4\text{ m s}^{-1}$ in China) at 0600 UTC on 30 June. Finally, it intensified into a typhoon (TY, with winds of $32.7\text{--}41.4\text{ m s}^{-1}$ in China), with a minimum sea level pressure of 970 hPa and maximum wind speed of 35 m s^{-1} (Figure 1(c) and (d)), and landed at Zhanjiang, Guangdong Province, causing tremendous damage in adjacent areas (Zhang *et al.*, 2008).

2.2. Numerical simulation

To examine the genesis process of TC Durian in detail, this study utilized a numerical simulation obtained using the Weather Research and Forecasting (WRF) model, version 3.5.1, driven by National Centers for Environmental Prediction (NCEP) reanalysis data, on $2.5^\circ \times 2.5^\circ$ grids. Based on the work in Zhang *et al.* (2008), the simulation used four nesting domains (displayed in Figure 1(a)) with horizontal resolutions of 54, 18, 6, and 1.2 km and mesh grids of 112×145 , 235×223 , 373×289 , and 951×776 , respectively. The Goddard microphysics scheme and Yonsei University boundary layer scheme were used in each domain, while the Kain–Fritsch cumulus parameterization scheme was only used in the two outermost domains. The model was initiated by analysis fields dominated by a monsoon trough, without a bogus vortex, and integrated for

84 h from 0000 UTC on 28 June to 1200 UTC on 1 July 2001. The two innermost domains started their integration 12 h after the initial time.

The model basically reproduced the large-scale circulation characteristics, including the position and evolution of the monsoon trough and the subtropical high (not shown). The simulated Durian was identified to generate at 0800 UTC on 29 June with the 6 km-resolution model data, when a system-scale low pressure center and the closed cyclonic circulation near the surface both first appeared (Figure 1(b)). The simulated track and intensity of Durian were compared with the best-track analysis of the Shanghai Typhoon Institute (<http://tcdatalyphoon.gov.cn/index.html>). The simulated track of Durian appeared to agree well with observations in the early stage of 0600 UTC on 29 June to 1200 UTC on 1 July (Figure 1(c)). The simulated genesis moment (0800 UTC on 29 June) of Durian was about 2 h later than observed (0600 UTC on 29 June), and the simulated formation location of Durian was $(116.2^\circ\text{E}, 16^\circ\text{N})$, which was about 80 km away from the observed location of $(117^\circ\text{E}, 16^\circ\text{N})$. The intensity errors reduced gradually as the circulation intensified (Figure 1(d)). The minimum sea level pressure decreased steadily from 0600 UTC on 29 June to 1200 UTC on 30 June and then decreased quickly from 1200 UTC on 30 June to 1200 UTC on 1 July. The observed Durian stably developed from a TD to a TS before 0600 UTC on 30 June 2001 and then rapidly intensified from a TS to a TY. The simulated maximum wind speed near the storm center was basically larger than the observed before 1800 UTC on 30 June, then the deviation significantly decreased. Even so, the wind speed of simulation and observation underwent a similar evolution trend.

Geostationary meteorological satellite (GMS) cloud images with a resolution of $0.05^\circ \times 0.05^\circ$, and simulated outgoing longwave radiation (OLR) with a resolution of 6 km, are presented in Figure 2. The incipient Durian cloud system evolved from a mesoscale cloud cluster, which was isolated from the north part of a mature mesoscale convective system (MCS, Figure 2). At 1800 UTC on 28 June, the disturbance in the north of the MCS developed into a mesoscale convective cloud (Figure 2(a)). Six hours later (0000 UTC on 29 June), the distribution of observed disturbance clouds became cyclonic (Figure 2(c)). After the moment of Durian's genesis (0600 UTC on 29 June), the cloud clusters grew larger and were better organized (Figure 2(e) and (g)). From the simulated OLR, a mesoscale cloud belt at the south of 15°N could be seen along the monsoon trough at 1800 UTC on 28 June. However, the convective cloud clusters had not yet organized, and were instead scattered irregularly at the north of the main cloud belt, possibly because the simulated mid-level vortex has not set up a proper condition to assist the organization of convection (Zhang and Bao, 1996a, 1996b). During the following period, a closed sea level pressure center developed. Meanwhile, the cloud clusters grew larger and generally organized into a tight, cyclonic system.

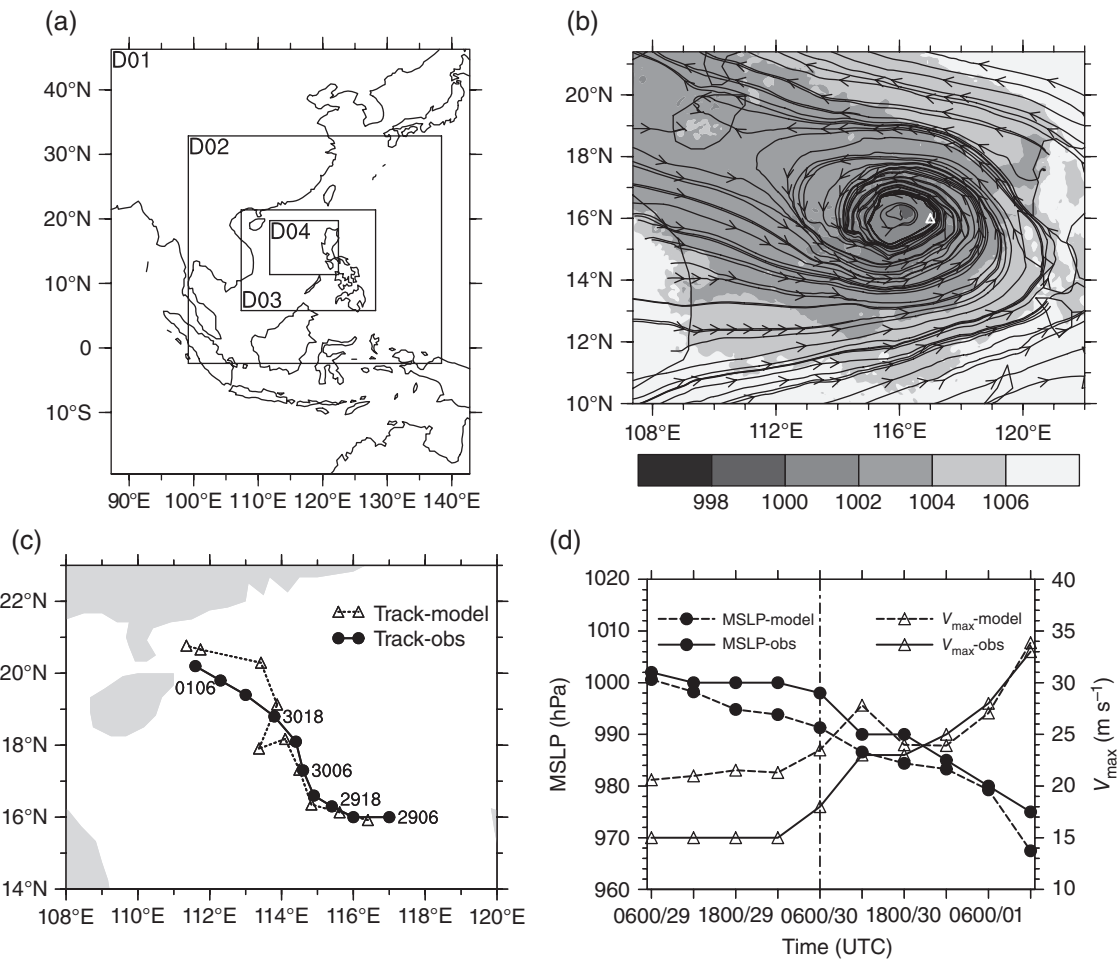


Figure 1. (a) Model domain configuration. (b) Streamlines at 900 hPa and sea level pressure (shaded, units: hPa) obtained from domain 3 at 0800 UTC on 29 June 2001. The triangle indicates the observed genesis location. (c) Track and (d) minimum sea level pressure (units: hPa) and maximum wind speed (units: m s^{-1}) of observed and simulated storms from 0600 UTC on 29 June to 1200 UTC on 1 July 2001. The interval is 6 h, and the vertical dashed line in (d) indicates the observed transition from a TD to a TS.

The success of the simulation, in terms of its reflection of the observed situation, justifies further examination of Durian's genesis process based on its results.

3. Multiscale features of Durian's genesis

3.1. Relative vorticity

Convection and vortices during TC genesis usually possess substantial and different-scale anomalous vorticity, and TC genesis is intimately linked to the enhancement of TC-scale cyclonic vorticity. The relative vorticity of domain 4, with grid spacing of 1.2 km at low [1 km above sea level (ASL)], middle (6 km ASL), and upper (11 km ASL) levels, was decomposed into three scales according to the spectral characteristics of the vorticity field: system scale (wavelengths >120 km), intermediate scale (wavelengths >30 km but <120 km), and small scale (wavelengths <30 km). The threshold values were selected based on the fact that the power spectra of the vorticity field at wavelengths <30 km, between 30 km and 120 km, and >120 km, exhibited different evolutions. The spectral decomposition was

obtained by a Fourier transform and filter, following Lin and Zhang (2008) and FZ11. The small-scale (convective-scale) relative vorticity centers are presumably induced by small-scale moist convection. Among them, those deep, rapidly rotating convective cores with horizontal scale of about 10–30 km are defined as VHTs, which usually develop a cyclonic vorticity bias at lower levels and appear as vorticity dipoles at middle–upper levels (Montgomery *et al.*, 2006). The VHTs have been demonstrated to exist in observation and play critical roles in TC genesis by numerical simulation analysis (Hendricks *et al.*, 2004; Montgomery *et al.*, 2006; Zhang *et al.*, 2008; Houze *et al.*, 2009). The intermediate-scale vorticity is regarded as a cluster of convective-scale vorticity, as that in FZ11.

Figure 3 presents the three-dimensional distribution of relative vorticity and its three scale components at 1800 UTC on 28 June (14 h prior to genesis), 0800 UTC on 29 June (the genesis moment), and 1800 UTC on 29 June (10 h after genesis). In general, the intensity of the small-scale vorticity was the strongest and the system-scale vorticity was the weakest (Figure 3). The small-scale vorticity

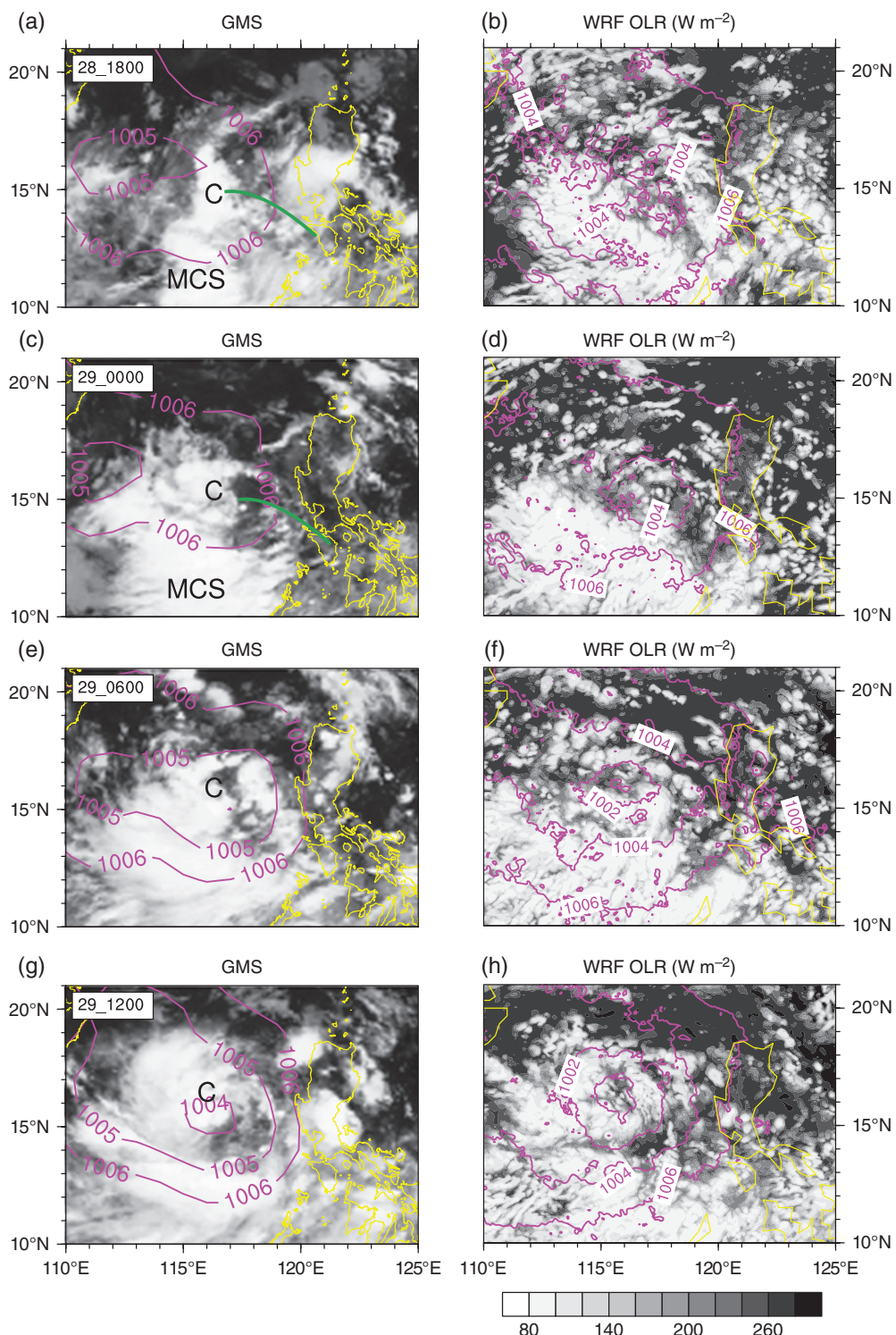


Figure 2. (a, c, e, g) GMS satellite images and mean sea level pressure (contours, units: hPa) from NCEP Final Operational Global Analysis data on a $1.0^\circ \times 1.0^\circ$ grid. (b, d, f, h) Simulated OLR (units: W m^{-2}) and sea level pressure (contours, units: hPa). (a, b) 1800 UTC on 28 June 2001; (c, d) 0000 UTC on 29 June 2001; (e, f) 0600 UTC on 29 June 2001; (g, h) 1200 UTC on 29 June 2001. MCS denotes mesoscale convective system; C denotes TC-related vortex; and the green line denotes the monsoon trough.

centers distributed irregularly inside and outside the 200 km-radius circular domain at 1800 UTC on 28 June (the fourth column in Figure 3(a)). The most intense small-scale vorticity anomalies were located at high levels near the tropopause. Fourteen hours later, at the genesis moment, low-level small-scale vorticity centers emerged and became stronger, tending

to aggregate radially inward in the genesis area and rotate anticyclonically (the fourth column in Figure 3(b)). Meanwhile, fewer small-scale vorticity centers existed at middle–upper levels with the TC’s formation. This coincided with a weakening of vertical velocity in the upper troposphere and a downward shift of vertical velocity cores (not shown). At 1800 UTC on 29 June

(10 hours after genesis), low-level small-scale and stronger vorticity centers were basically located within the 200 km-radius circular domain (the fourth column in Figure 3(c)). The aggregation of small-scale vorticity anomalies associated with VHTs and other small-scale convection is consistent with the analysis in Zhang *et al.* (2008); that is, a large number of VHTs occurred, while some of them as well as their residual vorticity aggregated and merged with each other. This phenomenon might be induced by larger-scale convergent or confluent flow, according to Fang and Zhang (2010). The intermediate-scale vorticity shared similar features of aggregation and development as the small-scale vorticity (the third column in Figure 3(a)–(c)). As for system-scale vorticity, a mid-level vortex, identified as the MCV according to Zhang *et al.* (2008), already existed at 1800 UTC on 28 June, and then became slightly weaker at the genesis moment. A relatively weak and well-organized low-level vorticity center, which represented the embryo of the storm, occurred at 0800 UTC on 29 June and subsequently intensified (the second column in Figure 3). In other words, the near-surface TC circulation had not been established until 0800 UTC on 29 June, and then it was able to self-develop.

3.2. Multiscale power spectra of relative vorticity

Figure 4 shows the integrated power spectra of relative vorticity at different levels, by adding up the power spectra at three different-scale ranges (FZ11). The scale separation has been carried out in a rectangular domain (400×400 km) moving with the mid-level vortex center (before genesis) and storm center (after genesis). The maximum amplitudes (spectral power) of small-scale and intermediate-scale vorticity were located in the upper troposphere at first, then decreased before 0600 UTC on 29 June and increased after 0600 UTC on 29 June with the genesis process of Durian (Figure 4(a), (b), and (f)). The maximum amplitudes of intermediate-scale vorticity moved downward from the upper troposphere to the middle troposphere. The center of system-scale spectral power existed at the middle level before 0300 UTC on 29 June, and then a low-level center gradually developed (Figure 4(c)). The low-level power spectra analysis shows that the amplitudes of the vorticity at the system scale (larger than 120 km) steadily increased, indicating that the near-surface TC circulation developed throughout Durian's genesis process. The amplitudes of the low-level vorticity at scales below 30 km was saturate and barely changed, while the power spectra of the intermediate-scale vorticity exhibited a slight decrease (Figure 4(d)). Furthermore, those amplitudes of the middle–upper-level vorticity at all scales showed a decreasing trend. Though the saturation of convective-scale vorticity may imply an immediate upscale transfer from the convective to the intermediate scale or system scale (FZ11), how the vorticity grows upscale remains an open question. Whether the transfer

of the maximum vorticity core from the middle troposphere to lower levels indicates a top-down mechanism is also a pending issue. The following section may provide some clues to these aspects via an analysis of the vorticity budget.

3.3. Sources of lower-to-middle tropospheric vorticity

The given analysis shows that the maximum system-scale vorticity gradually moved from the middle troposphere to the near surface during TC Durian's initial genesis process. To further evaluate the sources of different-level vorticity, a vorticity budget equation in a reference frame moving with the storm was solved, and the results are presented in this section. As shown in Davis and Galarneau (2009) and Raymond and López (2011), by integrating a traditional vorticity equation over any closed region and applying Gauss's theorem, the tendency of circulation around the area can be obtained (Raymond and López, 2011; Raymond *et al.*, 2011; Lussier *et al.*, 2014):

$$\frac{\partial \Gamma}{\partial t} = - \oint v_n \zeta_z dl + \oint \zeta_n v_z dl + \oint F_t dl \quad (1)$$

where Γ is the circulation; the line integrals are taken to be in the anticlockwise direction over the periphery of a horizontal area A ; v_n and ζ_n are the horizontal outward normal components of the velocity and relative vorticity; v_z and ζ_z are the vertical components of the velocity and absolute vorticity; and F_t is the component of frictional force \mathbf{F} tangential to the periphery of A in the direction of the integration. The term on the left hand side virtually represents the total vorticity tendency in area A . The first term on the right-hand side of Equation (1) is the vertical absolute vorticity flux on the periphery of A , representing the convergence of vorticity flux to the area A . The second term is referred to as a ‘tilting’ term here, which actually combines the tilting term with the vertical advection. Davis and Galarneau (2009) explicitly interpreted the relationship of this term with vortex tilting. The third term represents the spin-down tendency due to friction. The baroclinic generation term is omitted in Equation (1) since it is generally neglected (as in this TC genesis case) except in highly baroclinic environment such as the hurricane eyewall or mid-latitude fronts. More detail regarding the calculation method of these terms can be found in Raymond and López (2011).

Figure 5 represents the temporally averaged vertical profiles of the terms in Equation (1) in a 400 km-long box moving with the storm center. Results are expressed in terms of box-integral vorticity changes. The box contains the circulation centers in the lower-to-middle troposphere. Red lines denoted ‘net’ in Figure 5 indicate the sum of three terms on the right-hand side of Equation (1). During 1400–2000 UTC on 28 June

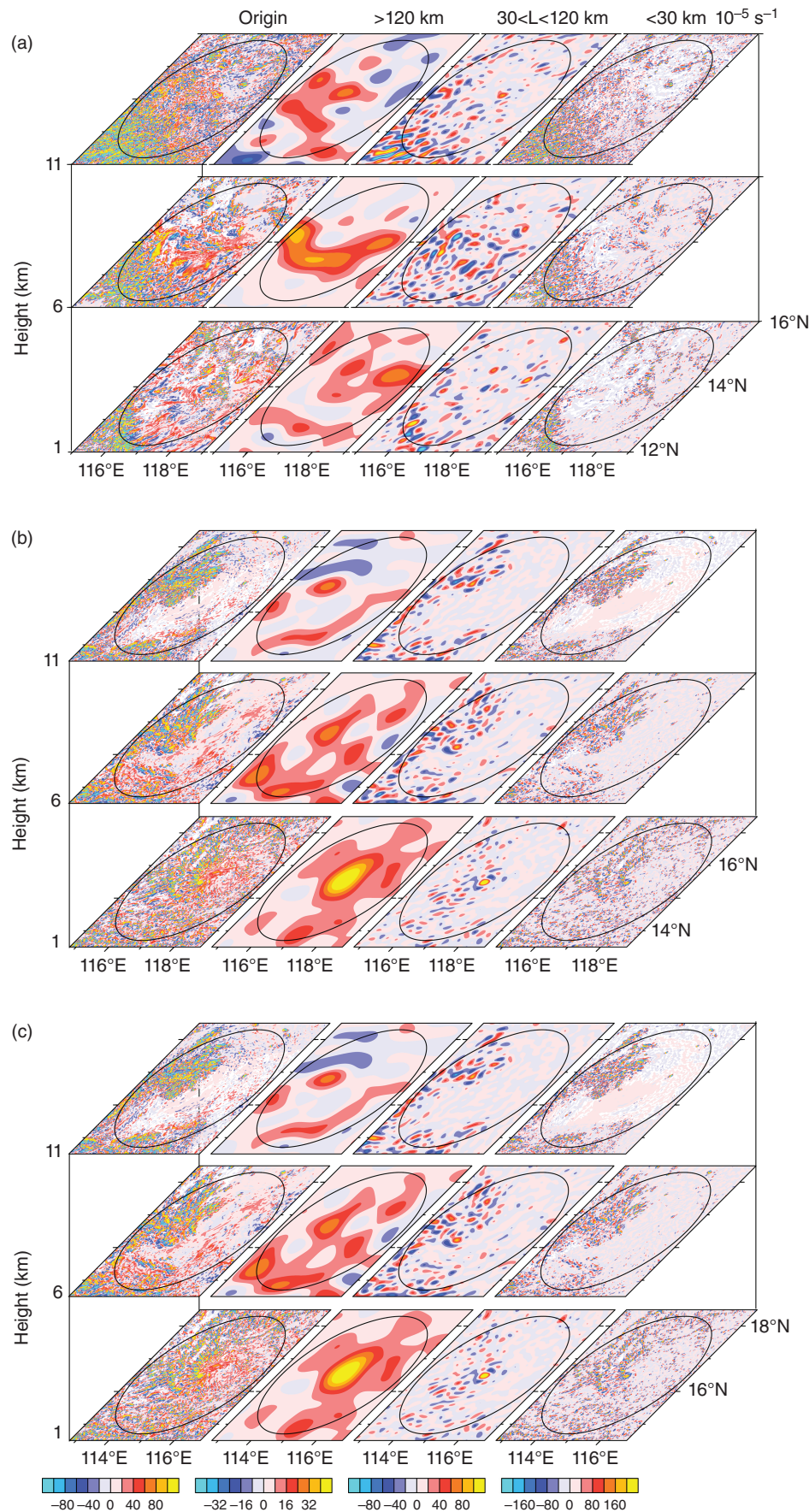


Figure 3. Horizontal distribution of low- ($z = 1 \text{ km}$), middle- ($z = 6 \text{ km}$), and upper-level ($z = 11 \text{ km}$) relative vorticity (shaded) at (a) 1800 UTC on 28 June, (b) 0800 UTC on 29 June, and (c) 1800 UTC on 29 June, of different scales: the original field (first column); scales $>120 \text{ km}$ (second column); scales between 30 and 120 km (third column); and scales $<30 \text{ km}$ (fourth column). Units: 10^{-5} s^{-1} . The solid-line circle indicates the 200 km-radius region around the circulation center.

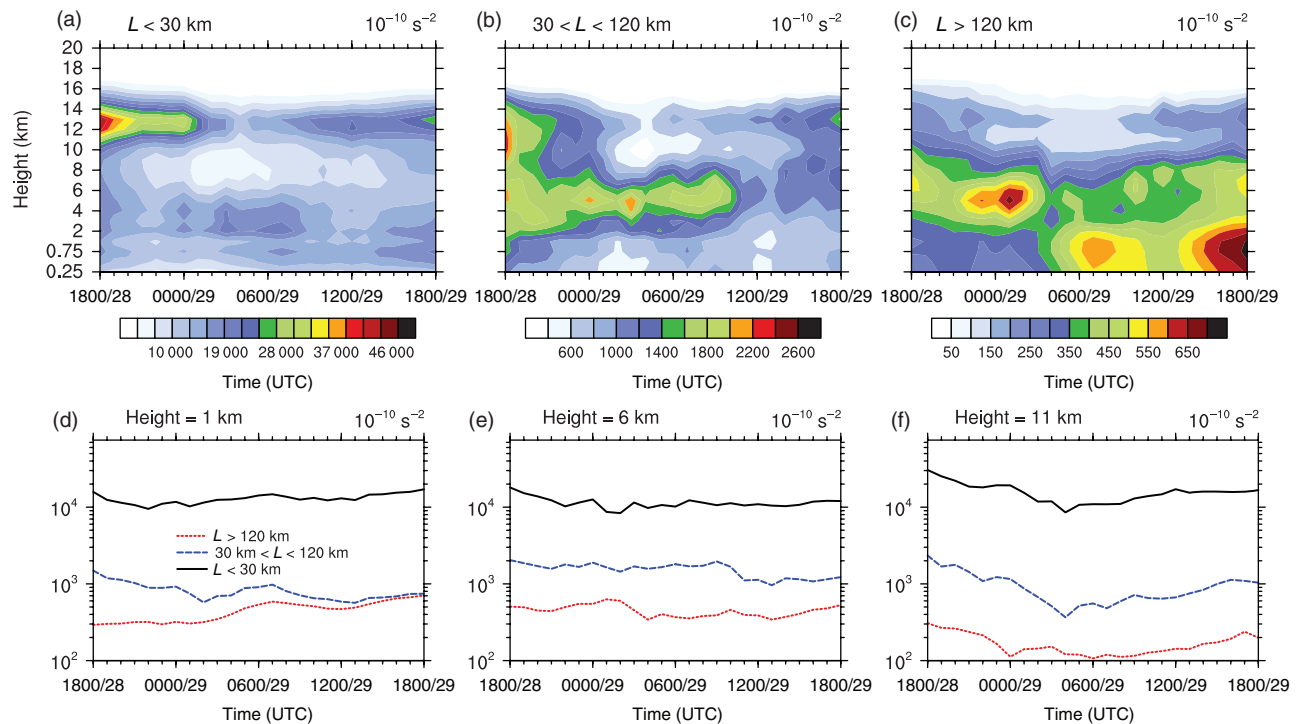


Figure 4. (a) Height–time cross section of the integrated power spectra of relative vorticity at the scale ranges $<30 \text{ km}$. Panels (b, c) as in (a), but for the scale ranges between 30 and 120 km, and scales $>120 \text{ km}$, respectively. (d) Temporal evolution of the integrated power spectra of relative vorticity at the three scale ranges at $z = 1 \text{ km}$. Panels (e, f) as in (d), but for $z = 6 \text{ km}$ and $z = 11 \text{ km}$, respectively. Units: 10^{-10} s^{-2} .

(18–12 h prior to genesis), vorticity increased throughout the whole troposphere. The circulation tendency at the lower-to-middle level was mainly due to the spin-up effect of vorticity flux convergence and the spin-down effect of the tilting term; while at the middle-to-upper level, the two effects were opposite. During 2000 UTC on 28 June to 0200 UTC on 29 June (12–6 h prior to genesis), the positive circulation tendency in the middle troposphere, corresponding to the development of the mid-level MCV, was contributed by both the convergence of vorticity flux and the tilting term. Friction almost offset the positive effect of convergence near the surface. During 0200–0800 UTC on 29 June (genesis moment), the middle-to-upper-level vorticity exhibited a significant decrease, which was induced by the divergence of vorticity flux above the planetary boundary layer (PBL). However, circulation still strengthened near the surface owing to the vorticity flux convergence, resulting in the system-scale vorticity center generally evolving from a mid-level vortex to a near-surface vortex. After Durian’s genesis (0800 UTC on 29 June 2001), positive circulation tendency recovered above the PBL due to the significant contribution of vortex tilting.

In general, the convergence of vertical vorticity flux and vortex tilting both played important roles in the circulation tendency. The accumulation of near-surface vorticity and the spin-up of the low-level vortex was mainly induced by the continuous vorticity flux convergence at the PBL. As for the vorticity in the middle-to-upper troposphere, the spin-up effect

of vortex tilting and the spin-down effect of vorticity flux convergence both worked. Meanwhile, the positive effect of vorticity flux convergence at the lower level, as well as the negative effect at the middle-to-upper level appears to have caused the shift of the system-scale vorticity center from the middle troposphere to the near surface.

4. Conclusions and discussion

In this study, TC Durian (2001), forming over the SCS, was simulated using the WRF model, and the model output data were compared with observations. The characteristics of multiscale vortices were then explored by separating the vertical relative vorticity into three scales: wavelength $<30 \text{ km}$, wavelength $>30 \text{ km}$ but $<120 \text{ km}$, and wavelength $>120 \text{ km}$.

The numerical simulation adequately reproduced the track and intensity of Durian, as well as its genesis process. The formation moment of the simulated TC was just 2 h later than observed, while the deviation of the formation location was about 80 km. The model was also capable of describing the organizational process of mesoscale cloud clusters during the formation.

In general, the smaller-scale vorticity was stronger than the larger-scale vorticity. As the TC generated, small-scale vorticity associated with VHTs and other convective-scale vortices tended to aggregate radially inward and rotate anticlockwise within the 200 km-radius circular domain. Meanwhile,

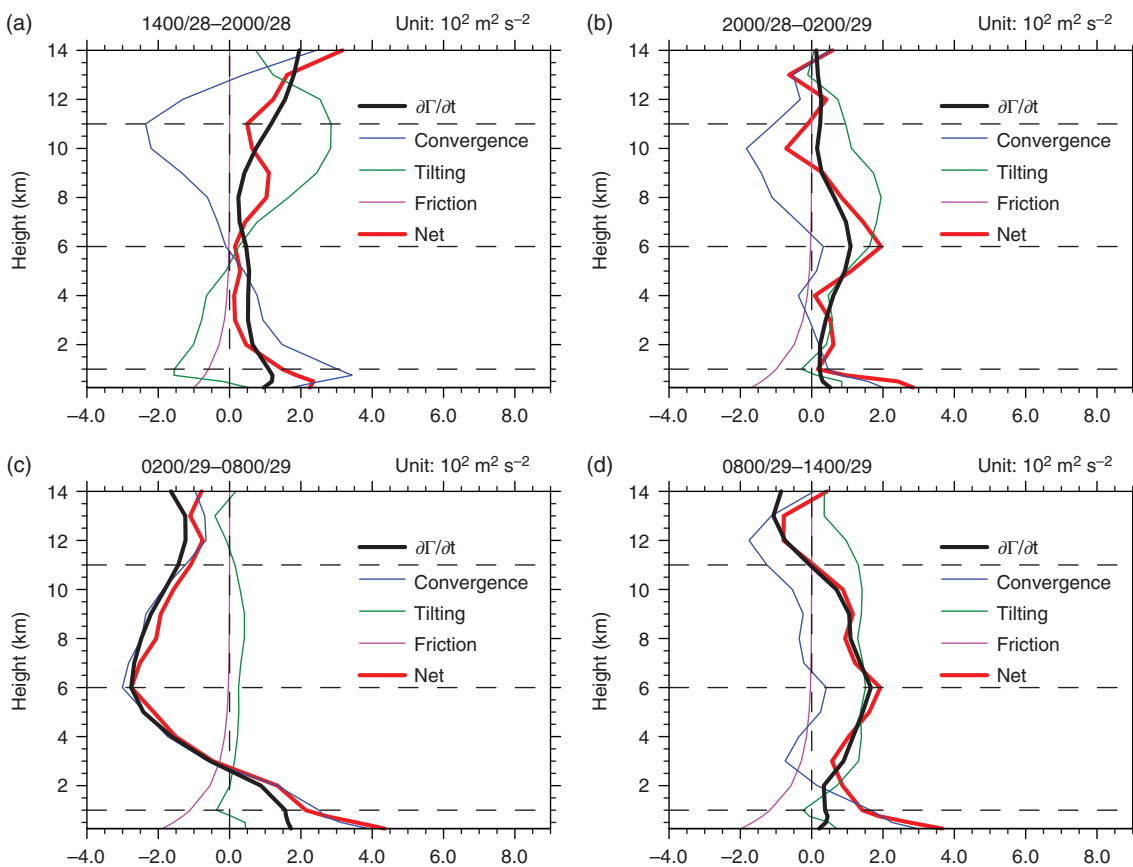


Figure 5. Vertical profiles of circulation budget terms averaged from (a) 1400 UTC on 28 June to 2000 UTC on 28 June, (b) 2000 UTC on 28 June to 0200 UTC on 29 June, (c) 0200 UTC on 29 June to 0800 UTC on 29 June, and (d) 0800 UTC on 29 June to 1400 UTC on 29 June, within a 400 km-long box moving with the storm: circulation tendency (black), contributions to the total circulation tendency (red) due to vorticity convergence (blue), vortex tilting (green), and friction (magenta) of Equation (1), units: $10^2 \text{ m}^2 \text{ s}^{-2}$. The three horizontal dashed lines denote 1, 6, and 11 km. The vertical dashed line denotes zero.

middle–upper level vorticity gradually weakened while low-level vorticity strengthened. Large-scale vorticity at the middle level before the simulated genesis moment (0800 UTC on 29 June 2001), and that at the low level after genesis, both possessed a well-organized center, representing the mid-level MCV and embryo of the TC, respectively. The power spectra analysis showed that the low-level disturbances at all scales <30 km barely changed, while the amplitudes at scales >120 km steadily increased. Analysis of the vorticity budget suggested that the development of low-level vorticity, or spin-up of near-surface circulation, was mainly caused by the convergence of the vertical vorticity flux. Meanwhile, the positive effect of low-level vorticity flux convergence and the negative effect of middle-to-upper-level convergence appear to have caused the shift of the system-scale vorticity center from the middle troposphere to the near surface.

Acknowledgements

The authors were supported by the National Basic Research Program of China (973 Program) under grant number 2015CB452804. The work was carried out at the National Supercomputer Center in Tianjin, and the calculations were performed on TianHe-1(A). The authors thank the two anonymous reviewers for their helpful comments on the manuscript.

References

- Bister M, Emanuel KA. 1997. The genesis of Hurricane Guillermo: TEXMEX analyses and a modeling study. *Monthly Weather Review* **125**: 2662–2682.
- Charney J, Eliassen A. 1964. On the growth of the hurricane depression. *Journal of the Atmospheric Sciences* **2**: 68–75.
- Cheung KKW. 2004. Large-scale environmental parameters associated with tropical cyclone formations in the western North Pacific. *Journal of Climate* **17**: 466–484.
- Davis CA, Ahijevych DA. 2012. Mesoscale structural evolution of three tropical weather systems observed during PREDICT. *Journal of the Atmospheric Sciences* **69**: 1284–1305.
- Davis CA, Galarneau TJ. 2009. The vertical structure of mesoscale convective vortices. *Journal of the Atmospheric Sciences* **66**: 686–704.
- Emanuel KA. 1986. An air-sea interaction theory for tropical cyclones. Part I: steady-state maintenance. *Journal of the Atmospheric Sciences* **43**: 585–605.
- Fang J, Zhang FQ. 2010. Initial development and genesis of Hurricane Dolly (2008). *Journal of the Atmospheric Sciences* **67**: 655–672.
- Fang J, Zhang FQ. 2011. Evolution of multiscale vortices in the development of Hurricane Dolly (2008). *Journal of the Atmospheric Sciences* **68**: 103–122.
- Gray WM. 1968. Global view of the origin of tropical disturbances and storms. *Monthly Weather Review* **96**: 669–700.
- Hendricks EA, Montgomery MT, Davis CA. 2004. The role of “vortical” hot towers in the formation of tropical cyclone Diana (1984). *Journal of the Atmospheric Sciences* **61**: 1209–1232.
- Houze RA, Lee WC, Bell MM. 2009. Convective contribution to the genesis of Hurricane Ophelia (2005). *Monthly Weather Review* **137**: 2778–2800.

- Lin Y, Zhang F. 2008. Tracking gravity waves in baroclinic jet-front systems. *Journal of the Atmospheric Sciences* **65**: 2402–2415.
- Lu XY, Cheung KKW, Duan YH. 2012. Numerical study on the formation of Typhoon Ketsana (2003). Part I: roles of the mesoscale convective systems. *Monthly Weather Review* **140**: 100–120.
- Lussier LL, Montgomery MT, Bell MM. 2014. The genesis of Typhoon Nuri as observed during the tropical cyclone structure 2008 (TCS-08) field experiment – part3: dynamics of low-level spin-up during the genesis. *Atmospheric Chemistry and Physics* **14**: 8795–8812.
- McBride JL, Zehr R. 1981. Observational analysis of tropical cyclone formation. Part II: comparison of non-developing versus developing systems. *Journal of the Atmospheric Sciences* **38**: 1132–1151.
- Montgomery M, Nicholls M, Cram T, Saunders A. 2006. A vortical hot tower route to tropical cyclogenesis. *Journal of the Atmospheric Sciences* **63**: 355–386.
- Palmen E. 1948. On the formation and structure of tropical hurricanes. *Geophysica* **3**: 26–38.
- Park M-S, Kim H-S, Ho C-H, Elsberry RL, Lee M-I. 2015. Tropical cyclone Mekkhala's (2008) formation over the South China Sea: mesoscale, synoptic-scale, and large-scale contributions. *Monthly Weather Review* **143**: 88–110.
- Raymond DJ, López CC. 2011. The vorticity budget of developing Typhoon Nuri (2008). *Atmospheric Chemistry and Physics* **11**: 147–163.
- Raymond DJ, Sessions SL, López CC. 2011. Thermodynamics of tropical cyclogenesis in the northwest Pacific. *Journal of Geophysical Research* **116**: D18101.
- Reasor PD, Montgomery MT, Bosart LF. 2005. Mesoscale observations of the genesis of Hurricane Dolly (1996). *Journal of Geophysical Research* **62**: 3151–3171.
- Riehl H. 1948. On the formation of typhoons. *Journal of Meteorology* **5**: 247–265.
- Ritchie EA, Holland GJ. 1997. Scale interactions during the formation of Typhoon Irving. *Monthly Weather Review* **125**: 1377–1396.
- Ritchie EA, Holland GJ. 1999. Large-scale patterns associated with tropical cyclogenesis in the western Pacific. *Monthly Weather Review* **127**: 2027–2043.
- Rotunno R, Emanuel KA. 1987. An air-sea interaction theory for tropical cyclones. Part II: evolutionary study using a nonhydrostatic axisymmetric numerical model. *Journal of the Atmospheric Sciences* **44**: 542–561.
- Sippel JA, Nielsen-Gammon JW, Allen SE. 2006. The multiple-vortex nature of tropical cyclogenesis. *Monthly Weather Review* **134**: 1796–1814.
- Zhang D-L, Bao N. 1996a. Oceanic cyclogenesis as induced by a mesoscale convective system moving offshore. Part I: a 90-h real-data simulation. *Monthly Weather Review* **124**: 1449–1469.
- Zhang D-L, Bao N. 1996b. Oceanic cyclogenesis as induced by a mesoscale convective system moving offshore. Part II: genesis and thermodynamic transformation. *Monthly Weather Review* **124**: 2206–2226.
- Zhang WL, Cui XP. 2013. Review of the studies on tropical cyclone genesis. *Journal of Tropical Meteorology* **29**: 337–346 (in Chinese).
- Zhang WL, Wang AS, Cui XP. 2008. The role of the middle tropospheric mesoscale vortex in the genesis of Typhoon Durian (2001) – simulation and verification. *Chinese Journal of Atmospheric Sciences* **32**: 1197–1209 (in Chinese).
- Zhang WL, Cui XP, Dong JX. 2010. The role of the middle tropospheric mesoscale vortex in the genesis of Typhoon Durian (2001) – diagnostic analysis of simulated data. *Chinese Journal of Atmospheric Sciences* **34**: 45–57 (in Chinese).
- Zhang GP, Cheung KKW, Lu XY. 2012. Numerical study on the formation of Typhoon Ketsana (2003) in the Western North Pacific. In 30th Conference on Hurricanes and Tropical Meteorology, FL, USA, 15–20 April 2012.